# Dynamics of multiphase flows via spectral boundary elements and parallel computations

Yechun Wang[a], Walter R. Dodson[a] and P. Dimitrakopoulos[a] * †

[a]Department of Chemical and Biomolecular Engineering,
University of Maryland, College Park, Maryland 20742, USA

We present the efforts of our research group to derive an optimized parallel algorithm for the efficient study of interfacial dynamics in Stokes flow and/or gravity. Our approach is based on our high-order/high-accuracy spectral boundary element methodology which exploits all the advantages of the spectral methods and the versatility of the finite element method. Our numerical code has been parallelized on shared-memory multiprocessor computers and thus we are able to utilize the computational power of supercomputers. Our parallel interfacial algorithm facilitates the study of a wide range of problems involving three-dimensional interfaces in Stokes flow and/or gravity.

## 1. INTRODUCTION

The dynamics of droplets and bubbles in infinite media or in restricted geometries under low-Reynolds-number flows and gravity is a problem of great technological and fundamental interest. These systems are encountered in a broad range of industrial, natural and physiological processes. Chemical engineering applications include enhanced oil recovery, coating operations, waste treatment and advanced materials processing. Pharmaceutical applications include emulsions which serve as a vehicle for the transport of the medical agent through the skin. An additional application is the blood flow in microvessels.

The industrial and biological applications of multiphase flows motivate the development of a parallel algorithm which can be employed to efficiently study the dynamics of three-dimensional interfacial problems. In this study we present the efforts of our research group to derive an optimized parallel algorithm for this problem based on a high-order/high-accuracy spectral boundary element methodology [1,2]. The main attraction of this approach is that it exploits all the benefits of the spectral methods (i.e. exponential convergence and numerical stability) and the versatility of the finite element method (i.e. the ability to handle the most complicated geometries) [3,4]. In addition, it is not affected by the disadvantage of the spectral methods used in volume discretizations; namely, the requirement to deal with dense systems, because in boundary integral formulations the resulting systems are always dense, independent of the form of discretization. The code

*Corresponding author, email: dimitrak@eng.umd.edu

†This work was supported in part by the National Science Foundation and the National Center for Supercomputing Applications (NCSA) in Illinois. Acknowledgment is made to the Donors of the American Chemical Society Petroleum Research Fund for partial support of this research.

has been parallelized on shared-memory supercomputers, such as the SGI Origin 2000, using OpenMP directives for the calculation of the system matrix, and highly optimized routines from the LAPACK system library for the solution of the dense system matrix. These properties result in a great computational efficiency which facilitates the study of a wide range of problems involving interfaces in Stokes flow.

## 2. MATHEMATICAL FORMULATION

We consider a three-dimensional fluid droplet in an infinite surrounding medium or a confined geometry; the droplet may be free-suspended or attached to the solid boundaries. The droplet size is specified by its volume $V_0$ or equivalently by the radius $a$ of a spherical droplet of volume $(4/3)\pi a^3 = V_0$. The droplet (fluid 1) has density $\rho_1$ and viscosity $\lambda\mu$, while the surrounding medium (fluid 2) has density $\rho_2$ and viscosity $\mu$. The gravitational acceleration is $g$, while the surface tension $\gamma$ is assumed constant. Far from the droplet, the flow approaches the undisturbed flow $\boldsymbol{u}^\infty$ (e.g. shear or Poiseuille flow) characterized by a shear rate $G$.

Excluding inertial forces, the governing equations in fluid 2 are the Stokes equations and continuity,

$$\boldsymbol{\nabla \cdot \sigma} = -\boldsymbol{\nabla} p + \mu \nabla^2 \boldsymbol{u} = 0 \tag{1}$$

$$\boldsymbol{\nabla \cdot u} = 0 \tag{2}$$

while in the droplet, the same equations apply with the viscosity replaced by $\lambda\mu$.

The boundary conditions on the solid walls and at infinity give

$$\boldsymbol{u} = 0 \quad \text{on} \quad \text{solid walls} \tag{3}$$

$$\boldsymbol{u} \to \boldsymbol{u}^\infty \quad \text{as} \quad r \to \infty \tag{4}$$

At the interface, the boundary conditions on the velocity $\boldsymbol{u}$ and surface stress $\boldsymbol{f}$ are

$$\boldsymbol{u}_1 = \boldsymbol{u}_2 \tag{5}$$

$$\boldsymbol{\Delta f} = \boldsymbol{f}_2 - \boldsymbol{f}_1 = \gamma(\boldsymbol{\nabla \cdot n})\boldsymbol{n} + (\rho_2 - \rho_1)(\boldsymbol{g \cdot x})\boldsymbol{n} \tag{6}$$

Here the subscripts designate quantities evaluated in fluids 1 and 2, respectively. The surface stress is defined as $\boldsymbol{f} = \boldsymbol{\sigma \cdot n}$, and $\boldsymbol{n}$ is the unit normal which we choose to point into fluid 2. The pressure as defined in $\boldsymbol{\sigma}$ is the dynamic pressure, hence the gravity force is absent from the Stokes equations and appears in the interfacial stress boundary condition.

For *transient* problems, the velocity field must satisfy an additional constraint - the kinematic condition at the interface

$$\frac{\mathrm{d}\boldsymbol{x}}{\mathrm{d}t} = (\boldsymbol{u \cdot n})\boldsymbol{n} \tag{7}$$

For *equilibrium shapes* under flow conditions and/or gravity, the kinematic condition at the interface becomes

$$(\boldsymbol{u \cdot n})\boldsymbol{n} = 0 \tag{8}$$

The magnitude of interfacial deformation due to viscous stress or gravity is given by the capillary number $Ca$ and Bond number $B_d$, respectively, which are defined by

$$Ca = \frac{\mu G a}{\gamma} \qquad B_d = \frac{(\rho_1 - \rho_2) g a^2}{\gamma} \tag{9}$$

Note that the capillary number $Ca$ represents the ratio of viscous forces to surface tension forces while the Bond number $B_d$ represents the ratio of gravitational forces to surface tension forces. The problem also depends on the viscosity ratio $\lambda$ and geometric dimensionless parameters in the case of solid boundaries. For fluid volumes in contact with solid substrates, additional conditions are required to prescribe the interface shape in the vicinity of the contact lines as discussed in our earlier publication [2]; these conditions introduce additional dimensionless parameters.

We emphasize that, although the governing equations and boundary conditions are linear in $\boldsymbol{u}$ and $\boldsymbol{f}$, the problem of determining interfacial shapes constitutes a nonlinear problem for the unknown interfacial shape; i.e. the velocity $\boldsymbol{u}$, stress $\boldsymbol{f}$ and curvature $\boldsymbol{\nabla \cdot n}$ are nonlinear functions of the geometrical variables describing the interface shape. For fluid volumes in contact with solid boundaries, the boundary conditions at the contact line involve the contact angle and thus constitute nonlinear functions of the unknown interfacial shape as well [2].

## 3. PARALLEL INTERFACIAL ALGORITHM

To solve the interfacial problem described in section 2, we transform the partial differential equations, Eqs.(1) and (2), which are valid in the system volume, into boundary integral equations valid on the surface of the volume [5,2]. This transformation results in a great reduction in CPU time, since a fully three-dimensional problem can be described and solved using only two (curvilinear) coordinates. For the case of a free-suspended droplet in an infinite medium, the velocity at a point $\boldsymbol{x}_0$ on the drop surface $S_B$ is given by

$$4\pi\mu(1+\lambda)\,\boldsymbol{u}(\boldsymbol{x}_0) - 4\pi\mu\,\boldsymbol{u}^{\infty}(\boldsymbol{x}_0) = \\ -\int_{S_B} \left[\boldsymbol{S}\cdot(\Delta\boldsymbol{f} - \boldsymbol{f}^{\infty}) - \mu\boldsymbol{T}\cdot((1-\lambda)\boldsymbol{u} - \boldsymbol{u}^{\infty})\cdot\boldsymbol{n}\right](\boldsymbol{x})\,\mathrm{d}S \tag{10}$$

where $\boldsymbol{S}$ is the fundamental solution for the three-dimensional Stokes equations and $\boldsymbol{T}$ the associated stress defined by

$$S_{ij} = \frac{\delta_{ij}}{r} + \frac{\hat{x}_i\hat{x}_j}{r^3} \qquad T_{ijk} = -6\frac{\hat{x}_i\hat{x}_j\hat{x}_k}{r^5} \tag{11}$$

where $\hat{\boldsymbol{x}} = \boldsymbol{x} - \boldsymbol{x}_0$ and $r = |\hat{\boldsymbol{x}}|$. Similar equations hold in the presence of solid boundaries and for drop suspensions [2,6].

In contrast to most researchers in this area who employ low-order methods (e.g. see [7–10]), we solve the resulting boundary integral equations employing a (high-order) spectral boundary element method [1,2]. In particular, each boundary is divided into a moderate number of spectral elements as shown in Figure 1. On each element the geometric and physical variables are discretized using Lagrangian interpolation based on the zeros of

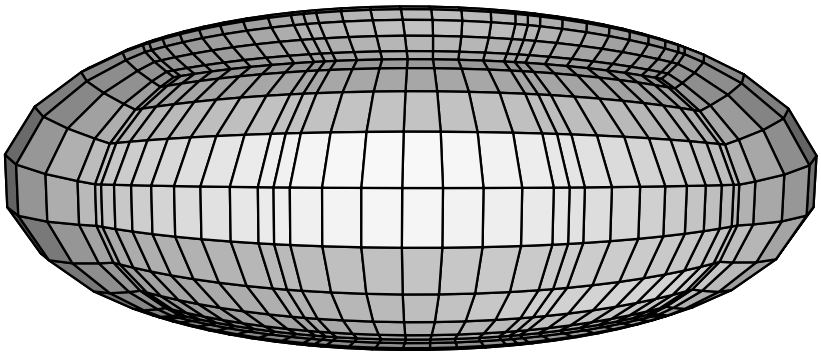

Figure 1. Discretization of a drop surface into $N_E = 14$ spectral elements. The figure illustrates Gauss-Lobatto Legendre distribution of nodal lines with $N_B = 10$ spectral points in each direction.

orthogonal polynomials of Gauss or Gauss-Lobatto type [3]. This is equivalent to an orthogonal polynomial expansion and yields the spectral convergence associated with such expansions. The discretizations are substituted into the appropriate boundary integrals and quadratures evaluated using adaptive Gaussian quadrature.

In order to determine equilibrium fluid interfaces in Stokes flow and/or gravity, we have developed an efficient, Jacobian-free, Newton method based on our spectral boundary element method. This method has proved to be a robust algorithm, of high accuracy and extreme efficiency, valid to study the most complicated three-dimensional problems [2]. To determine transient interfacial shapes, we combine our optimized parallel spectral boundary element algorithm with a time integration of the kinematic condition at the interface, Eq.(7).

The main attraction of our interfacial algorithm is the fact that it exploits all the benefits of the spectral methods, i.e. exponential convergence and numerical stability with the versatility of the finite element method, i.e. the ability to handle the most complicated geometries. In addition, it is not affected by the disadvantage of the spectral methods used in volume discretization; namely, the requirement of dealing with dense systems, because in boundary integral formulations the resulting systems are always dense, independent of the form of the discretization.

We emphasize that our interfacial algorithm shows the exponential convergence of the spectral methodology in any interfacial problem. For example, the exponential convergence in the numerical accuracy as the number of the employed spectral points $N = N_E\, N_B^2$ increases is clearly evident at the geometric properties of a given shape such as the computed curvature shown in Figure 2. The difference in the accuracy between our spectral algorithm and low-order interpolation methods is dramatic. For example, Zinchenko, Rother and Davis [8] in their Figure 5 reported an error $\approx 4 \times 10^{-2}$ for $N = 5120$; our algorithm shows an error $\approx 1 \times 10^{-10}$ for $N = 3456$.

To be able to access the computational power of supercomputers, our numerical code has been parallelized on shared-memory multiprocessor computers (such as the SGI Origin 2000) by employing OpenMP directives for the calculation of the system matrix, and

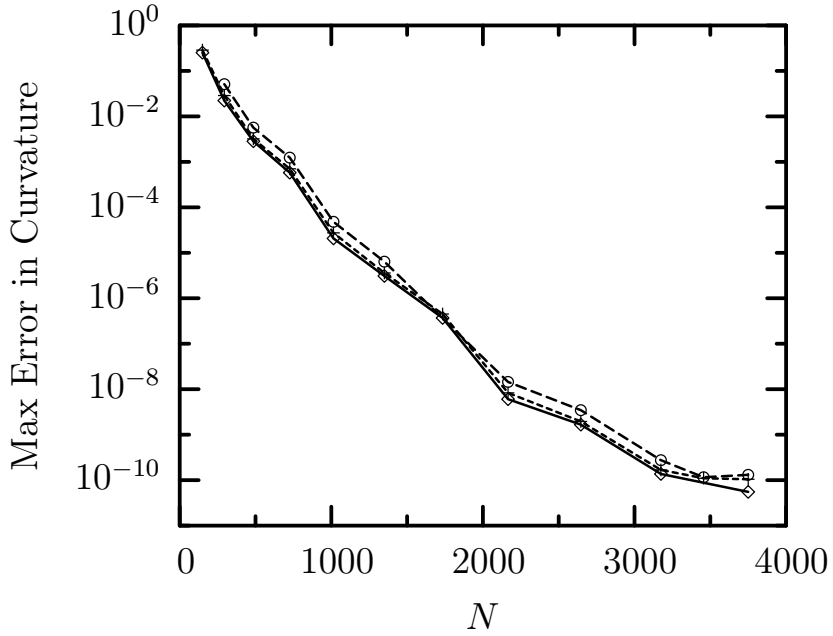


Figure 2. Exponential convergence in the maximum absolute error of the computed curvature as the number of spectral points $N$ increases for different spheroids: ——, $a = b = c = 1$; - - - -, $a = b = 1, c = 0.4$; – – – –, $a = 1, b = c = 0.4$.

highly optimized routines from the LAPACK system library for the solution of the dense system matrix. Multiprocessor runs exploit the parallel nature of calculating the system matrices described by the boundary integral equation, Eq.(10). This results in an overall very good parallel efficiency as shown in Table 1. We emphasize that the size of the problems tested is rather small involving 10–40 spectral elements. Higher efficiency is expected for more complicated problems such as the ones involving the interaction of many droplets.

We emphasize that, to be able to achieve the parallel properties shown in Table 1, it is imperative that the computational load is distributed evenly among the processors. For this, we distribute the load using an "interleave" schedule with a small chunk size, e.g. we set the environmental variable `OMP_SCHEDULE` to `STATIC,1` (see OpenMP API [11]). On the other hand, an uneven load can result in poor parallel performance. For example, a "simple" schedule which divides the load into large chunks based on the number of iterations in the associated `OMP PARALLEL DO` loop produces an efficiency of nearly 75% for the "Integration" on two processors which is much smaller than the optimal efficiency of 99.26% shown in Table 1. Non-optimal load distribution also worsens the efficiency of the systems' solution, i.e. the performance of the parallel LAPACK library.

The parallelization of our algorithm can be performed in two ways: the first way involves all the spectral points on each element while the second one involves all the spectral points on all elements. Considering that each element has $N_B \times N_B$ spectral points (with a typical value of $N_B = 10$) while $N_E$ is the number of the spectral elements (with a typical value of $N_E$ =10–40 for problems with one droplet and much higher values for many-drop

Table 1
Efficiency versus the number of processors $N_p$ for the calculation ("Integration") and the solution ("Solution") of the system matrices resulting from our parallel spectral boundary element algorithm on the shared-memory SGI Origin 2000 provided by the National Center for Supercomputing Applications (NCSA) in Illinois. Note that efficiency denotes the ratio of the wall time for the serial execution $T_s$ to that for the parallel execution $T_p$ multiplied by the number of processors, i.e. efficiency $\equiv T_s/(T_p\,N_p)$.

| $N_p$ | Integration (%) | Solution (%) |
|---|---|---|
| 1 | 100.00 | 100.00 |
| 2 | 99.26 | 89.62 |
| 4 | 96.72 | 75.43 |
| 8 | 89.91 | 72.34 |

problems), it is easy to realize that by employing the first way of parallelization we may use a moderate number of processors while by employing the second way of parallelization we have the ability to exploit a very high number of processors, if available. For many-drop problems (i.e. study of emulsions and foams), the parallelization can also involve the different drops/bubbles (or teams of them).

To optimize further our algorithm we employ highly-optimized BLAS routines as well as cache optimization. Exploiting the levels $n$ of symmetry of a problem reduces the memory requirements by a factor of $2^n$, the computational time for the system matrices by a factor of $2n$ and the time for the direct solution of the linear systems by factor of $2^n$.

With this optimized parallel algorithm, we have the ability to study in detail a wide range of problems involving fully three-dimensional interfaces in Stokes flow and/or gravity. For example, in Figure 3 we provide the interfacial dynamics for viscosity ratio $\lambda = 0.2$ in a planar extensional flow near the critical conditions, i.e. near the flow rate at which equilibrium interfacial shapes cease to exist. The critical capillary number (i.e. $Ca \approx 0.155$) is in excellent agreement with experimental findings [12]. Observe that below the critical flow rate, the droplet deformation reaches equilibrium while above it the droplet continues to deform with time.

## 4. CONCLUSIONS

In this paper, we have presented the efforts of our research group to derive an optimized parallel algorithm so that we are able to efficiently determine interfacial dynamics in Stokes flow and/or gravity. By employing the boundary integral formulation, the problem dimensionality is reduced by one. In addition, our high-order/high-accuracy spectral boundary element approach results in great benefits including exponential convergence, numerical stability and ability to handle the most complicated geometries. The exponential convergence of our spectral methodology results in additional savings in computational time since for a desired accuracy we can use a coarser grid compared to that employed by low-order boundary methods. Our numerical code has been parallelized on shared-memory supercomputers, such as the SGI Origin 2000, using OpenMP directives

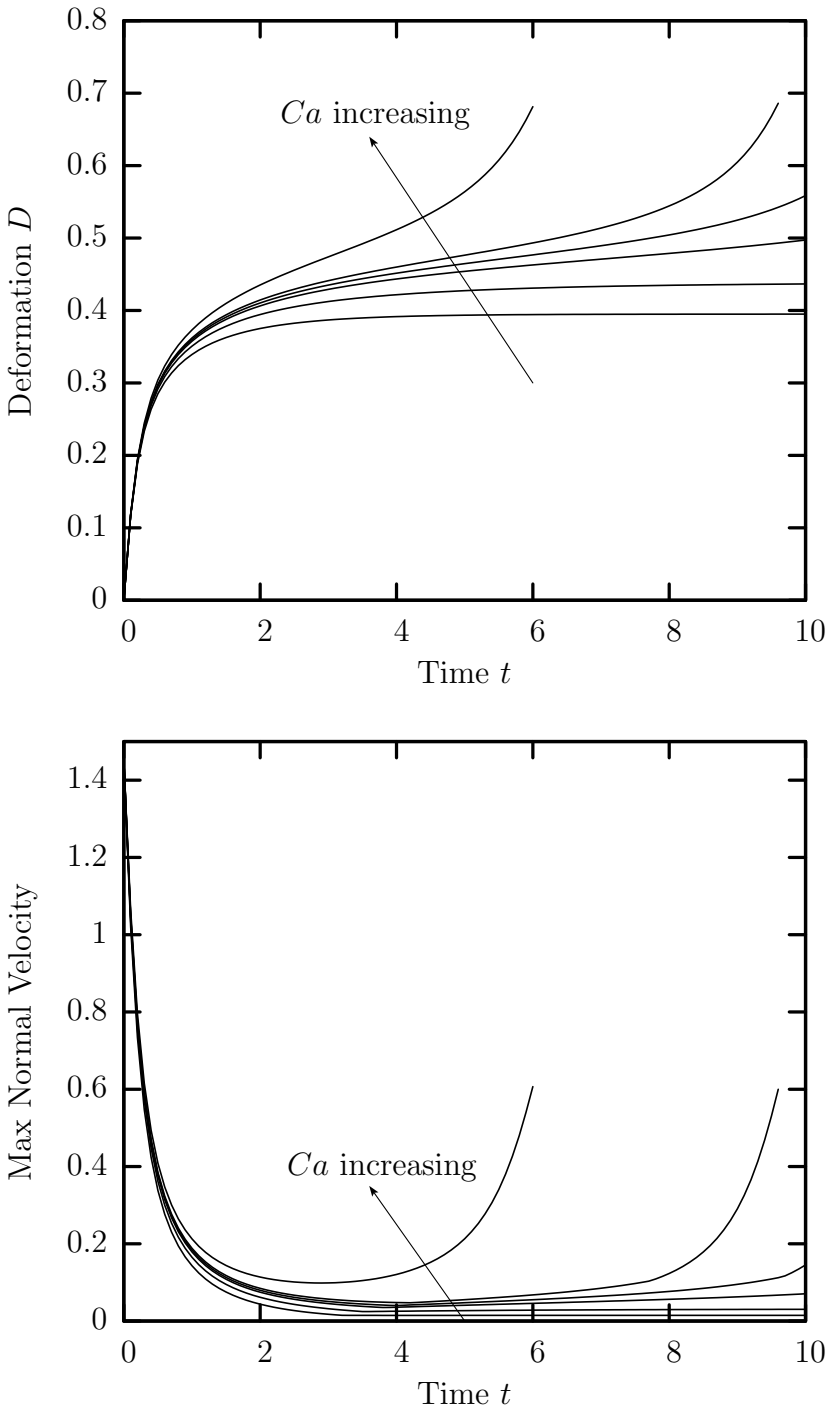


Figure 3. Dynamics near the critical point for a droplet with viscosity ratio $\lambda = 0.2$ in a planar extensional flow $\boldsymbol{u}^\infty = G\,(x, -y, 0)$. $(a)$ Droplet deformation $D$ versus time $t$. $(b)$ Maximum normal velocity versus time $t$. The capillary number is $Ca = 0.15, 0.155, 0.158, 0.159, 0.16, 0.165$. Note that $D \equiv (L - S)/(L + S)$ where $L$ and $S$ are the droplet's length and width, respectively.

for the calculation of the system matrix, and highly optimized routines from the LAPACK system library for the solution of the system matrices. This enables us to utilize the computational power available at supercomputer centers including the National Center for Supercomputing Applications (NCSA) in Illinois. All these properties result in a great computational efficiency which facilitates the study of a wide range of problems involving fully three-dimensional interfaces in Stokes flow and/or gravity.

## REFERENCES

1. G. P. Muldowney and J. J. L. Higdon, J. Fluid Mech. 298 (1995) 167.
2. P. Dimitrakopoulos and J. J. L. Higdon, J. Fluid Mech. 377 (1998) 189.
3. C. Canuto, M. Y. Hussaini, A. Quarteroni and T. A. Zang, Spectral Methods in Fluid Dynamics, Springer, 1988.
4. Y. Maday and A. T. Patera, in State of the Art Surveys in Computational Mechanics, A. K. Noor and J. T. Oden (eds.), ASME, 1989.
5. C. Pozrikidis, Boundary Integral and Singularity Methods for Linearized Viscous Flow, Cambridge University Press, 1992.
6. A. Z. Zinchenko and R. H. Davis, J. Fluid Mech. 455 (2002) 21.
7. M. Loewenberg and E. J. Hinch, J. Fluid Mech. 321 (1996) 395.
8. A. Z. Zinchenko, M. A. Rother and R. H. Davis, Phys. Fluids 9 (1997) 1493.
9. C. Pozrikidis, J. Comp. Phys. 169 (2001) 250.
10. I. B. Bazhlekov, P. D. Anderson and H. E. H. Meijer, Phys. Fluids 16 (2004) 1064.
11. OpenMP Architecture Review Board (eds.), OpenMP Application Program Interface, 2005 (available at `http://www.openmp.org`).
12. B. J. Bentley and L. G. Leal, J. Fluid Mech. 167 (1986) 241.